Histol Histopathol (2026) 41: 439-452

Histology and Histopathology
From Cell Biology to Tissue Engineering

ORIGINAL ARTICLE Open Access

SLMO2 inhibits apoptosis in ovarian cancer cells by modulating mitochondrial function via TRIAP1

Yaqi Wang[1], Yuesong Wang[1], Zixuan Li[2] and Tianmei Zhang[1]

[1]Department of Gynecology, Yantaishan Hospital and [2]Binzhou Medical University, Yantai, Shandong, PR China

Summary. Objective. This study aimed to investigate the role of SLMO2 in regulating mitochondrial function and its interaction with TRIAP1, which inhibited apoptosis in ovarian cancer cells. The findings provided valuable insights into potential therapeutic targets for ovarian cancer.

Methods. Lentiviral infection models were developed using SKOV3 and OVCAR3 ovarian cancer cell lines. Techniques such as flow cytometry, western blotting, immunofluorescence, and transmission electron microscopy were employed to systematically assess the regulatory effects of SLMO2 and TRIAP1 on cell proliferation, apoptosis, mitochondrial function, and autophagy. Additionally, a subcutaneous mouse tumor xenograft model was utilized to further investigate the combined effects of SLMO2 and TRIAP1 on ovarian cancer cells, with the aim of elucidating the specific mechanisms underlying tumor growth and apoptosis.

Results. SLMO2 enhanced mitochondrial function by increasing membrane potential and reducing reactive oxygen species (ROS) levels. Furthermore, through its interaction with TRIAP1, SLMO2 inhibited autophagy, which further suppressed apoptosis in ovarian cancer cells and regulated mitochondrial function. *In vivo* experiments showed decreased ROS levels and reduced expression of autophagy-related proteins, further supporting the roles of SLMO2 and TRIAP1 in the regulation of mitochondrial function.

Conclusions. SLMO2 regulated mitochondrial function and inhibited apoptosis in ovarian cancer cells by interacting with TRIAP1. The combination of SLMO2 and TRIAP1 promoted tumor cell growth and induced oxidative stress, suggesting potential therapeutic targets for ovarian cancer.

Key words: SLMO2-TRIAP1, Ovarian cancer, Mitochondrial function, Apoptosis inhibition

Corresponding Author: Tianmei Zhang, No.10087, Science and Technology Avenue, Laishan District, Yantai City, 264003, Shandong Province, PR China. e-mail: ytsztm@163.com

www.hh.um.es. DOI: 10.14670/HH-18-958

Introduction

Ovarian cancer is one of the leading causes of cancer-related deaths among women worldwide. Although its incidence is relatively low, the mortality rate remains high (Penny, 2020). According to the 2022 edition of the Global Cancer Statistics Report, there were 19.96 million new cancer cases and 9.74 million cancer deaths worldwide. The incidence, prevalence, and mortality rates of ovarian cancer have been increasing annually (Bray et al., 2024). In recent years, the rapid advancements in molecular biology and cell biology have increasingly highlighted the role of mitochondria in tumorigenesis and development (Luo et al., 2020). Mitochondria are not only the centers of cellular energy metabolism, they are also extensively involved in cell proliferation, apoptosis, oxidative stress, and various other biological processes (Vringer and Tait, 2022; Zhang et al., 2023; Liu et al., 2024a). Studies have demonstrated that various mutations in mitochondrial DNA (mtDNA) are present in ovarian cancer tissues (Kopinski et al., 2021). These mutations may impair mitochondrial function and further promote the proliferation and metastasis of tumor cells (Smits et al., 2023). Therefore, comprehensive studies of mitochondrial mechanisms in ovarian cancer are crucial for enhancing diagnostic accuracy and treatment efficacy in this disease.

Slowmo Homolog 2 (SLMO2), also referred to as PRELI Domain Containing 3B (PRELID3B), is a lipid transporter primarily responsible for the translocation of phosphatidylserine from the cytoplasm to the inner mitochondrial membrane (Miyata et al., 2022). It plays a crucial role in regulating mitochondrial function by interacting with other proteins to modulate processes such as mitochondrial membrane potential, anti-apoptotic effect, and energy metabolism (Dee and Moffat, 2005). Studies have demonstrated that SLMO2 is significantly upregulated in various tumors, particularly in ovarian, breast, and lung cancers. High expression levels of this protein are associated with poorer patient outcomes and increased tumor aggressiveness (Liu et al., 2024b). This suggested that SLMO2 may facilitate rapid tumor growth and

metastasis by maintaining mito-chondrial function and regulating energy metabolism.

TP53-regulated apoptosis suppressor 1 (TRIAP1) is a protein-coding gene involved in various biological processes (Nedara et al., 2022). It is primarily located in the inner mitochondrial membrane and serves to protect cells during apoptosis. Studies have demonstrated that the interaction between SLMO2 and TRIAP1 forms a complex within the cell, acting as a novel lipid transfer protein in the mitochondria. This complex enhances the anti-apoptotic capabilities of mitochondria, enabling cancer cells to survive and proliferate under oxidative stress or other pro-apoptotic conditions (Aaltonen et al., 2016; Miliara et al., 2019). Therefore, to elucidate the pathogenesis of ovarian cancer and identify potential therapeutic targets, this study investigated the expression of SLMO2 in ovarian cancer cells using both *in viv*o and *in vitro* models. Additionally, it examined the relationship between the inhibitory effect of SLMO2 on apoptosis in ovarian cancer apoptosis and mitochondrial function. We conducted a comprehensive investigation into the downstream molecular mechanisms.

Materials and methods

Cell culture

The human ovarian cancer cell line SKOV3 (CBP60291, Cobioer, CHN) was cultured in the appropriate complete culture medium. The OVCAR3 cell line (CBP60294, Cobioer, CHN) was cultured in the appropriate complete culture medium. Both cell cultures were maintained at 37°C in an atmosphere of 5% CO_2.

Cell grouping

Group 1: The logarithmic growth phases of SKOV3 and OVCAR3 cells were divided into five distinct groups. The study included the Control, sh-SLMO2, sh-SLMO2 negative control (sh-SLMO2-NC), OE-SLMO2, and OE-SLMO2 negative control (OE-SLMO2-NC) groups. The cells in the control group received no treatment. Other groups received lentiviral transfections of OE-SLMO2, OE-SLMO2-NC, sh-SLMO2, and sh-SLMO2-NC.

Group 2: The logarithmic growth phase of SKOV3 cells was divided into six distinct groups. The study included the Control, OE-SLMO2, OE-SLMO2 and sh-TRIAP1 (OE-SLMO2+sh-TRIAP1), OE-SLMO2 and sh-TRIAP1 negative control (OE-SLMO2+sh-TRIAP1-NC), OE-SLMO2 and OE-TRIAP1 (OE-SLMO2+OE-TRIAP1), and OE-SLMO2 and OE-TRIAP1 negative control (OE-SLMO2+OE-TRIAP1-NC) groups. The cells in the control group received no treatment. Other groups received lentiviral transfections of OE-SLMO2, sh-TRIAP1, sh-TRIAP1-NC, OE-TRIAP1, and OE-TRIAP1-NC.

Cell infection

The day prior to transfection, 5×10^4 cells in the logarithmic growth phase were seeded into 24-well plates. The cells were cultured overnight at 37°C, and the cell density was expected to reach approximately 50% confluency the following day. The original culture medium was aspirated, and the cells were gently washed twice with phosphate-buffered saline (PBS, ST447-1L, Beyotime, CHN). The cells were subsequently infected with 5 μg/mL polybrene and 5×10^6 TU/mL lentivirus (Genomeditech, CHN), achieving a multiplicity of infection (MOI) value of 10. After 24 hours of infection, the medium containing the lentivirus was removed, and the culture was continued for an additional 48 hours with fresh medium.

The target gene sequences of the lentivirus were as follows:

sh-SLMO2:5' GCATGATATGTCAGGTTATTT 3'
sh-SLMO2-NC:5' GAATATGTTTATCGGTCTAGT 3'
OE-SLMO2:NC_000020.11 (59033145…59042786, complement)
OE-SLMO2-NC:5' GATACGATGCACCCTAATATA 3'
sh-TRIAP1:5' GCGTGGAATCAGCTTTACATA 3'
sh-TRIAP1-NC:5' GGATTCATCGCTCGAAATGTA 3'
OE-TRIAP1:NC_000012.12 (120443964…120446384, complement)
OE-TRIAP1-NC:5' GCTCGAATATGGCTAATACGT 3'

Cell Counting Kit-8 (CCK-8) detection

Transfected cells were seeded into 96-well plates at a density of 2.5×10^4 cells per 100 μL and cultured for 24 hours. After incubation, 10 μL of CCK-8 reagent (CK04, DOJINDO LABORATORIES, JPN) was added to each well, and the plates were incubated at 37°C for 2 hours. Cell viability was assessed by measuring the absorbance at 450 nm using a SpectraMax Gemini XPS (Molecular Devices, USA).

Flow cytometry

Apoptosis Rate: Cells were collected and centrifuged at 800 g for 5 minutes. The cells were washed twice with PBS and gently resuspended in 500 μL binding buffer to obtain a single-cell suspension. The suspension was mixed with 5 μL Annexin V-FITC (C10492, Thermo Fisher, USA), and 5 μL propidium iodide. The mixture was incubated at room temperature, protected from light, for 10 minutes. Flow cytometry (NovoCyte, Agilent, USA) was then used for detection.

Mitochondrial Membrane Potential Detection (JC-1): The JC-1 dye (T3168, Thermo Fisher, USA) was prepared in a suitable buffer. A 0.5 mL working solution of JC-1 was added to the cell suspension and incubated at 37°C in a 5% CO_2 atmosphere for 30 minutes to facilitate dye uptake by the mitochondria. After incubation, the working solution was removed through

centrifugation, and the cells were washed once with a buffer solution. The stained cells were subsequently re-suspended in the buffer and analyzed using flow cytometry.

Reactive Oxygen Species (ROS) Assay: DCFH-DA (HY-D0940, MCE, USA) was diluted 1:1000 in serum-free medium to achieve a final concentration of 10 μM. The working solution was added to the cell suspension and incubated at 37°C with 5% CO_2 for 30 minutes, allowing the probe to penetrate the cells and be hydrolyzed by intracellular esterases. After incubation, the solution was removed through centrifugation, and the cells were washed once with a buffer. The cells were subsequently resuspended in PBS, and ROS levels were measured using flow cytometry.

Immunofluorescence staining (IF)

Cells were seeded onto slides at approximately 70% confluency. After cell attachment, 100 μL of permeabilization solution (G1204, ServiceBio, CHN) was added, and the slides were incubated at room temperature for 20 minutes. The slides were then washed twice with PBS. Blocking solution (P0102, Beyotime, CHN) was added, and the slides were incubated at room temperature for 2 hours. Subsequently, the slides were incubated overnight at 4°C with a primary antibody against SLMO2 (C31989, 1:200, SAB, USA). On the following day, the slides were incubated with the second antibody (AS011, 1:200, Abclonal, CHN) at room temperature for 1 hour. Mitochondria were labeled using MitoTracker®Red CMXROS (40741ES50, 1:250, Yeasen, CHN) at room temperature for 30 minutes. Nuclear staining was then performed using 4',6-diamidino-2-phenylindole (DAPI, 62248, Thermo Fisher, USA) for 10 minutes. After staining, the slides were mounted with an anti-fading reagent (P36980, Thermo Fisher, USA). Images were captured using a fluorescence microscope (DMi8S, Leica, GER).

Transmission Electron Microscope (TEM)

Cells were centrifuged and fixed with glutaraldehyde (G6257, Sigma, GER). The cells were washed three times with 0.1 M phosphate buffer (P3813, Sigma, GER) for 20 minutes each time. Then, 2% osmium tetroxide (O5500, Sigma, GER) was added, and fixation was carried out for 1.5 hours. The cells were washed twice with phosphate buffer for 5 minutes each time. Next, the cells were dehydrated through a series of ethanol gradients and then treated with anhydrous acetone (904082, Sigma, GER) for 15 minutes at 4°C. After overnight embedding, ultrathin sections (70 nm) were cut and stained with 2% uranyl acetate (U25690, Shanghai Acmec Biochemical Technology Co., Ltd., CHN) and lead citrate (L26640, Shanghai Acmec Biochemical Technology Co., Ltd., CHN). Transmission electron microscopy was used for observation and imaging.

Animals

Four-week-old SPF-grade female nude mice (18-22 g) were provided by Jinan Pengyue Experimental Animal Breeding Co., Ltd. (SCXK(Lu)2022 0006, CHN). The mice were housed at a temperature of (21±2) °C, with a humidity of 50%±5%, under a natural circadian rhythm, and had free access to food and water. All animal experiments were conducted in accordance with the guidelines set forth by the hospital's Animal Ethics Committee and received approval. The study adhered to EU regulations regarding the care and use of laboratory animals and complied with the ARRIVE guidelines for reporting animal research.

In this study, twenty nude mice were randomly divided into four groups of five mice: the Control, OE-SLMO2, OE-SLMO2+sh-TRIAP1, and OE-SLMO2+ OE-TRIAP1 groups. A subcutaneous tumor model was established by injecting transfected SKOV3 cells (1×10^7 cells) subcutaneously into the right axilla of each mouse. After 28 days, the nude mice were anesthetized with 3% pentobarbital sodium and euthanized by cervical dislocation. The tumors were excised and weighed. Portions of the tumor tissue were fixed in 4% paraformaldehyde (P0099, Beyotime, CHN), while the remaining tissue was stored in liquid nitrogen for subsequent analysis.

Tumor volume was measured weekly using the formula: $\text{Volume}=\text{Length}\times\text{Width}^2\times0.5$

Dihydroethidium (DHE) detection of ROS

Fresh, unfixed tissue was sectioned into 10-μm-thick frozen slices. To prepare the sections, 200 μL of cleaning solution was added and allowed to sit at room temperature for 5 minutes. After removing the cleaning solution, 100 μL of the DHE dye working solution (HR9069, Bjbalb, CHN) was applied, and the sections were incubated at 37°C for 60 minutes in the dark. The staining solution was subsequently removed, and the sections were washed twice with PBS. Nuclear staining was conducted by adding DAPI (GDP1024, ServiceBio, CHN), followed by a 10-minute incubation at room temperature. After removing DAPI and washing the sections twice with PBS, they were mounted using glycerin. Images were captured using a fluorescence microscope (DMi8S, Leica, GER).

Immunohistochemical staining (IHC)

After embedding the tissue in paraffin, 4-μm sections were cut, dewaxed with xylene, and gradually rehydrated with ethanol. The tissue sections were incubated at room temperature with 3% H_2O_2 (88597, Merck, USA) for 20 minutes to block endogenous peroxidase activity. Antigen retrieval was performed by boiling the sections in a water bath for 5 minutes. After naturally cooling to room temperature, the sections were blocked with 5% BSA (V9009, Sigma, USA) and then

incubated overnight at 4°C with the diluted antibodies (Ki-67, 12202, 1:200, CST, USA; SLMO2, C31989, 1:200, SAB, USA; TRIAP1, orb40236, 1:200, Biorbyt, UK). On the following day, the sections were washed and incubated with horseradish peroxidase (HRP)-conjugated secondary antibody (8114, 1:200, CST, USA) for 1 hour at room temperature. The sections were then stained with diaminobenzidine (DAB) staining solution (P0202, Beyotime, CHN) for 10 minutes, rinsed with water, and counterstained with hematoxylin (C0107, Beyotime, CHN) for 3 minutes. The sections were removed, soaked in water, and then placed in hydrochloric acid for dehydration, followed by immediate immersion in water for 5 minutes. Dehydration and clearing were performed using a graded ethanol solution. The slides were then mounted, and protein expression was observed under a microscope (CX31, OLYMPUS, JP). Image analysis was conducted using ImageJ software. All tissue sections were independently reviewed and scored in a blinded manner by two experienced pathologists. The final score was determined by averaging the two evaluations to ensure the objectivity and consistency of the results.

Western blot analysis

Cells or tissues were lysed, and the lysates were centrifuged at 12,000 rpm for 10 minutes at 4°C to collect the supernatant. Protein concentration was determined using the Bicinchoninic Acid (BCA) Protein Assay Kit (P0012, Beyotime, CHN). Samples (20 μg of protein) were denatured at 100°C for 10 minutes, then separated by SDS-PAGE and transferred onto polyvinylidene fluoride (PVDF) membranes (88520, Thermo Fisher, USA). The membranes were blocked with 5% skim milk in TBST at 4°C for 2 hours. After blocking, the membranes were incubated overnight at 4°C with the following primary antibodies: SLMO2 (orb2308297, 1:1000, Biorbyt, UK), Beclin-1 (MA5-15825, 1:500, Thermo Fisher, USA), Parkin (ab315376, 1:1000, Abcam, UK), Pink1 (ab300623, 1:1000, Abcam, UK), TRIAP1 (PA5-76211, 1:1000, Thermo Fisher, USA), Bax (ab3191, 1:1000, Abcam, UK), Bcl-2 (ab182858, 1:2000, Abcam, UK), Cleaved Caspase-3 (ab32042, 1:500, Abcam, UK), and β-actin (ab8226, 1:1000, Abcam, UK). After washing with TBST, the membranes were incubated with species-specific HRP-conjugated secondary antibodies (ab288151, 1:5000, Abcam, UK; ab6728, 1:5000, Abcam, UK) for 2 hours at room temperature. Protein bands were visualized using enhanced chemiluminescence (ECL) detection reagents (A38554, Thermo Fisher, USA) and captured with a Tanon 4600 imaging system (Tanon, CHN). Band intensity was quantified using ImageJ software.

Data and statistical analysis

Data were analyzed using GraphPad Prism version 8.0 software. Results were presented as the mean ± standard error of the mean (SEM). The normality of the data was assessed using the Shapiro-Wilk test, and group comparisons were conducted using the appropriate statistical tests. For comparisons between two groups, independent sample t-tests were employed when the data followed a normal distribution. For multiple group comparisons, a one-way analysis of variance (ANOVA) was conducted, followed by *post-hoc* tests as needed. Non-parametric tests, such as the Mann-Whitney U test and the Kruskal-Wallis test, were employed when the data did not conform to a normal distribution. A p-value of less than 0.05 ($p<0.05$) was considered statistically significant.

Results

SLMO2 expression promoted cell proliferation and inhibited apoptosis

To investigate the effect of SLMO2 expression on ovarian cancer cells, we developed SKOV3 and OVCAR3 cell models featuring both SLMO2 knockdown and overexpression. Lentiviral infection was confirmed through western blot analysis, which demonstrated successful knockdown of SLMO2 and its overexpression in both SKOV3 and OVCAR3 cells (Fig. 1A-C). Compared with the Control group, the knockdown of SLMO2 significantly inhibited the proliferation of ovarian cancer cells, whereas the overexpression of SLMO2 significantly promoted cell proliferation (Fig. 1D, E). Meanwhile, the knockdown of SLMO2 can promote apoptosis in ovarian cancer cells, whereas the overexpression of SLMO2 significantly inhibits cell apoptosis (Fig. 1F-H). Immunofluorescence results revealed that SLMO2 was expressed in the mitochondria of SKOV3 and OVCAR3 cells (Fig. 1I).

SLMO2 expression enhanced mitochondrial function in cells

A decrease in mitochondrial membrane potential is a hallmark of early apoptosis. To further investigate the impact of SLMO2 on mitochondrial function in ovarian cancer cells, we assessed changes in mitochondrial membrane potential using flow cytometry. Results indicated that, compared with the control group, JC-1 monomers were significantly increased in the sh-SLMO2 group, suggesting a decrease in mitochondrial membrane potential (Fig. 2A-C). In contrast, in the OE-SLMO2 group, JC-1 aggregates formed within the mitochondrial matrix, leading to a significant increase in membrane potential. Additionally, ROS play a crucial role in various physiological and pathological processes, including cell growth, proliferation, differentiation, aging, and apoptosis. Measurement of intracellular ROS levels revealed a significant increase in the sh-SLMO2 group, while the OE-SLMO2 group exhibited a significant decrease (Fig. 2 D-F). These results suggest that SLMO2 enhances mitochondrial function in SKOV3 and OVCAR3 cells by increasing mitochondrial membrane potential and reducing reactive ROS levels, thereby inhibiting apoptosis.

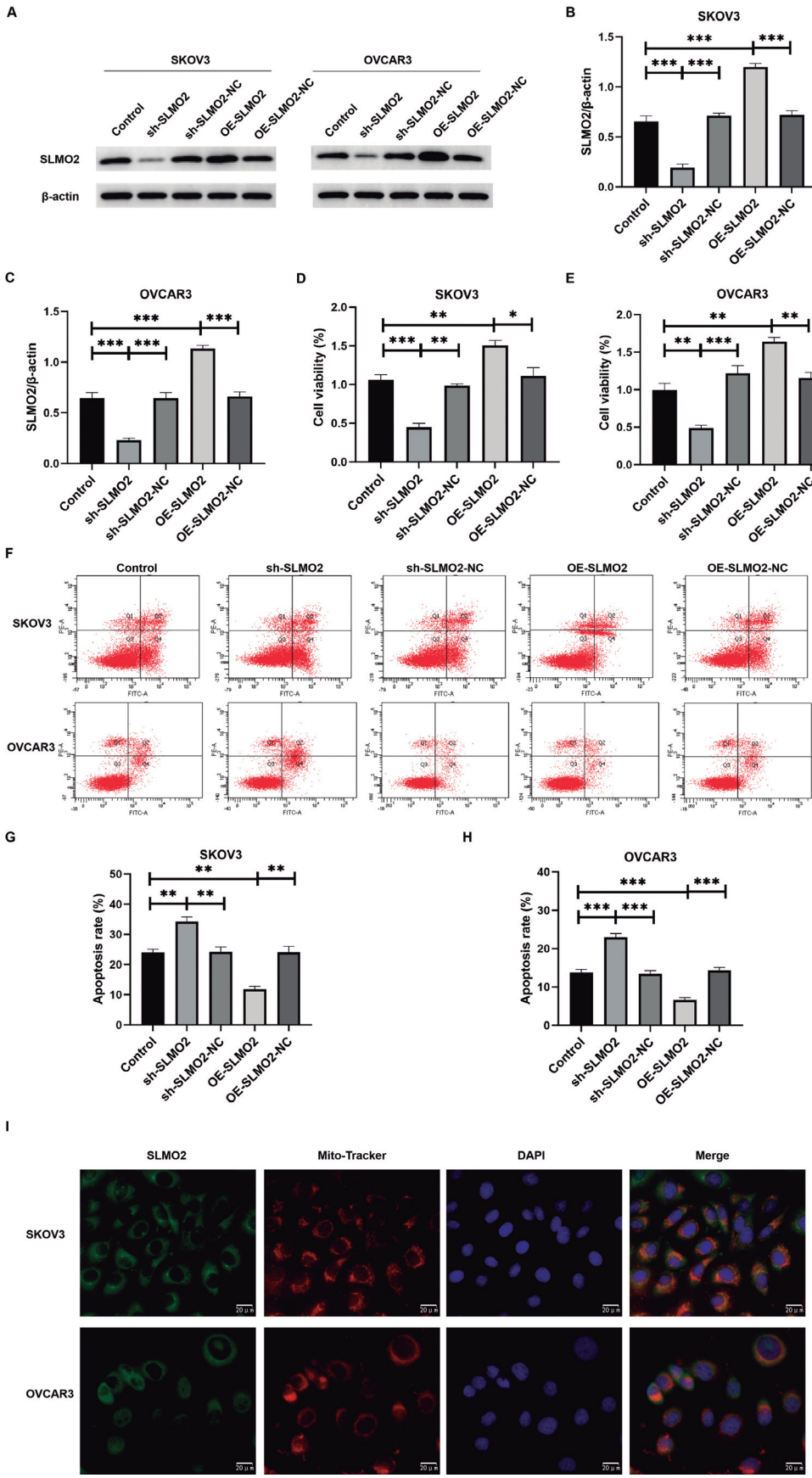

Fig. 1. SLMO2 expression promoted cell proliferation and inhibited apoptosis. **A-C.** Western blot was performed to confirm transfection efficiency, and ImageJ was utilized for the quantitative analysis of protein band intensities. **D, E.** The CCK8 assay was utilized to assess the impact of SLMO2 overexpression on the proliferation of SKOV3 and OVCAR3 cells. **F-H.** Flow cytometry was utilized to assess the impact of SLMO2 overexpression on apoptosis in SKOV3 and OVCAR3 cells. **I.** Immunofluorescence was utilized to examine the localization of SLMO2 within the mitochondria of SKOV3 and OVCAR3 cells. n=3, **p*<0.05, ***p*<0.01, ****p*<0.001. Scale bars: 20 μm.

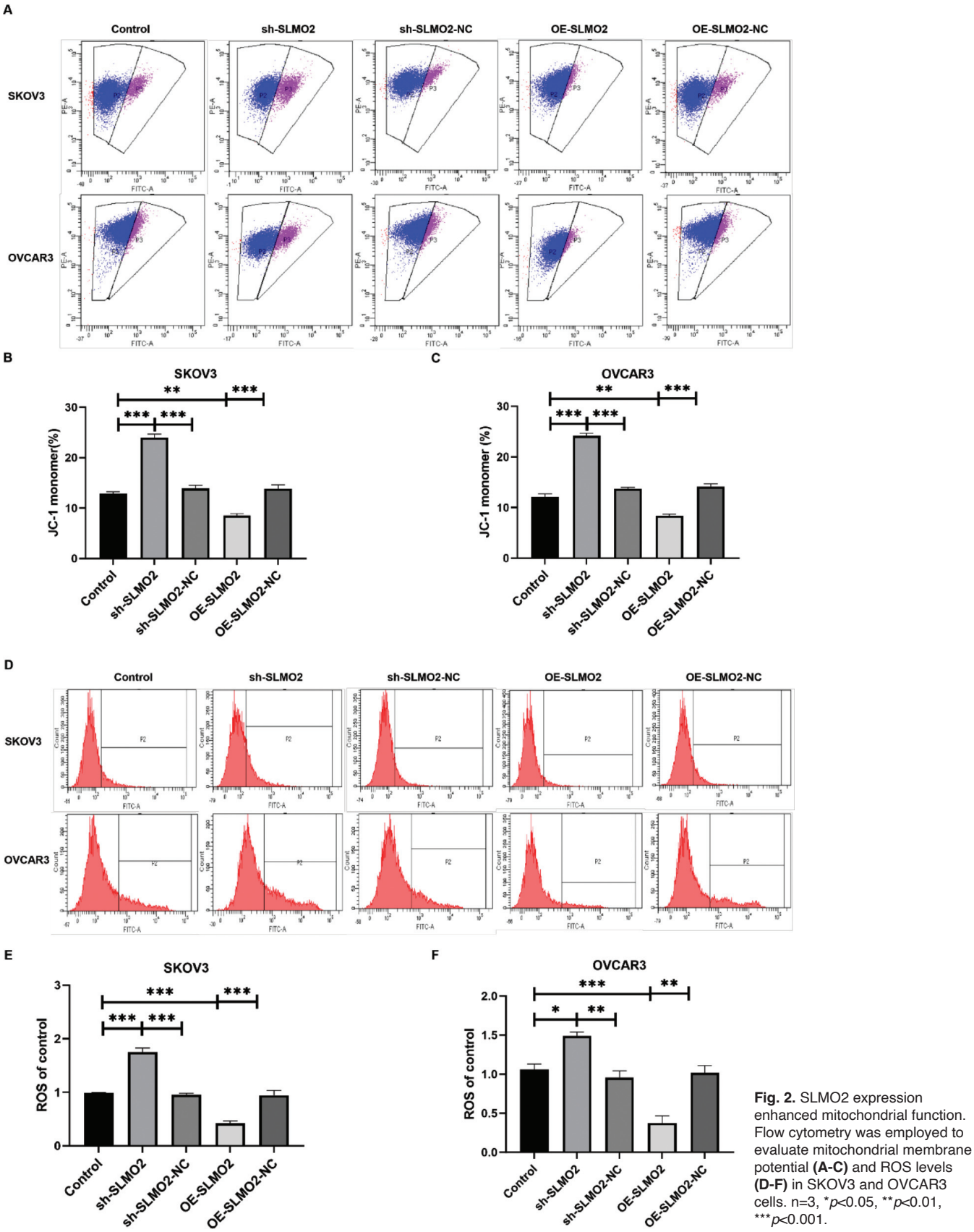

Fig. 2. SLMO2 expression enhanced mitochondrial function. Flow cytometry was employed to evaluate mitochondrial membrane potential **(A-C)** and ROS levels **(D-F)** in SKOV3 and OVCAR3 cells. n=3, *p<0.05, **p<0.01, ***p<0.001.

SLMO2 expression inhibited autophagy in cells

To further investigate the effects of SLMO2 on autophagy and mitochondrial homeostasis, we analyzed mitochondrial structure and morphology using TEM. Results indicated that in the sh-SLMO2 group, the formation of mitochondrial autophagosomes was induced, mitochondria exhibited significant swelling, and cristae were disorganized, fragmented, or even absent. SLMO2 overexpression inhibited mitochondrial autophagy (Fig. 3A). Additionally, western blot analysis was performed to evaluate the expression levels of proteins related to autophagy and mitochondrial function. The results indicated that the expression levels of Beclin-1, Parkin, and Pink1 were significantly increased following the knockdown of SLMO2. Conversely, the overexpression of SLMO2 led to a significant reduction in the expression of these proteins (Fig. 3B-E). These findings indicated that SLMO2 expression suppresses autophagy in cells.

SLMO2 targeted TRIAP1 to promote ovarian cancer

Studies have demonstrated that SLMO2 binds to TRIAP1, forming complexes that act as novel lipid transfer proteins within mitochondria. In this study, we overexpressed SLMO2 in SKOV3 cells using lentiviral infection, followed by the knockdown and overexpression of TRIAP1 to further investigate their effects on ovarian cancer cells. SKOV3 cells were chosen for their high transfection efficiency, stable gene expression profile, and well-documented use in studies of apoptosis and mitochondrial function, making them an ideal model for mechanistic exploration. The western blot results

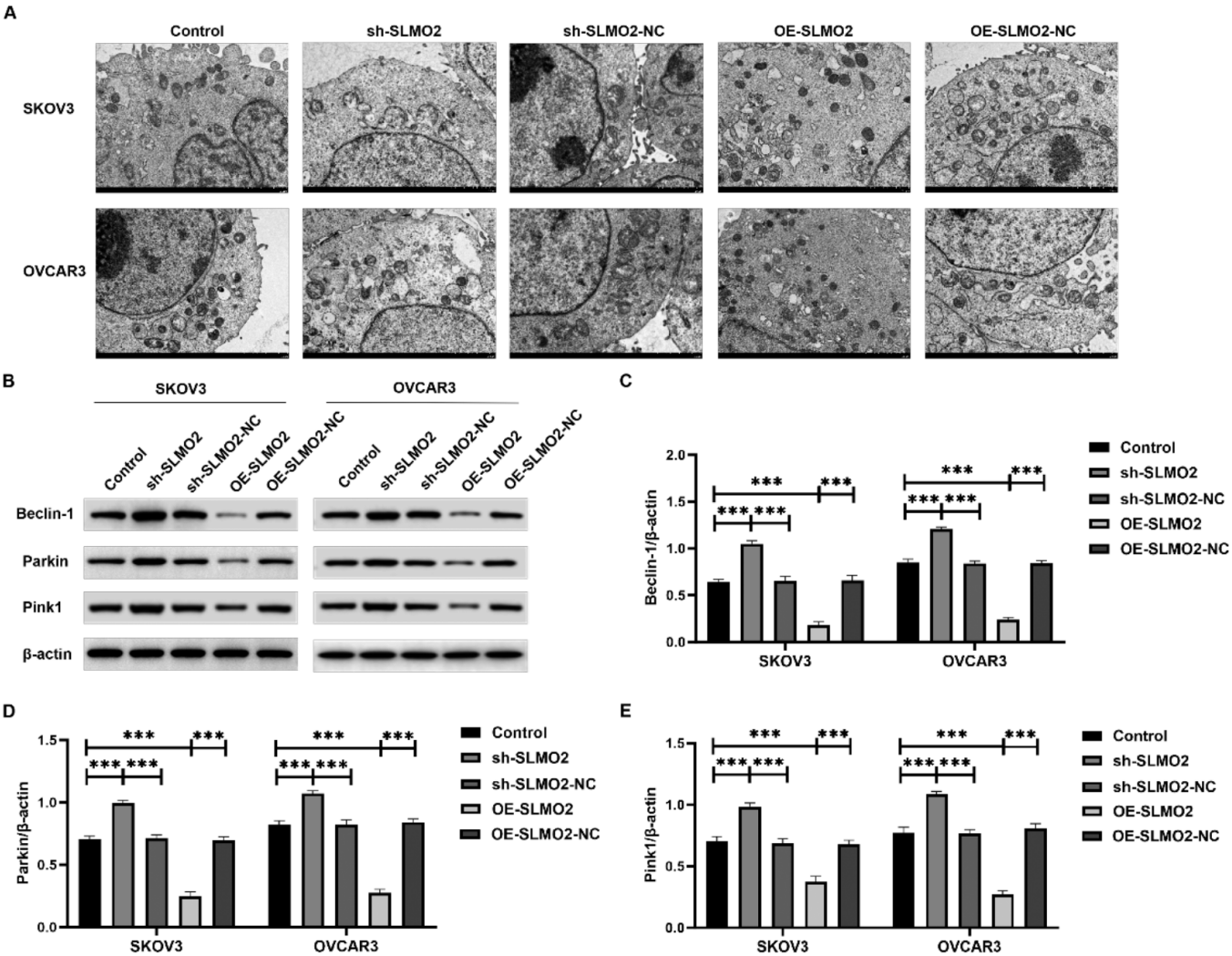

Fig. 3. SLMO2 expression inhibited cellular autophagy. **A.** TEM was employed to observe the ultrastructure of mitochondria. **B-E.** Western blot analysis was conducted to detect the expression of proteins associated with autophagy and mitochondrial function. This was followed by a quantitative analysis of protein band intensities using ImageJ. n=3, $^{**}p<0.01$, $^{***}p<0.001$. x 2500.

confirmed the successful expression of SLMO2 and TRIAP1 in SKOV3 cells (Fig. 4A-C). Flow cytometry was utilized to evaluate apoptosis. Compared with the OE-SLMO2 group, the OE-SLMO2+sh-TRIAP1 group significantly increased cell apoptosis, whereas the OE-SLMO2+OE-TRIAP1 group significantly reduced cell apoptosis (Fig. 4D,E). Furthermore, western blot analysis of apoptosis-related proteins, including Bax, Bcl-2, and cleaved caspase-3, revealed that the OE-SLMO2+sh-TRIAP1 group enhanced the expression of these proteins, while the OE-SLMO2+OE-TRIAP1 group significantly reduced their expression (Fig. 4 F-I). These findings suggest that SLMO2 targets TRIAP1 to promote ovarian cancer in SKOV3 cells.

SLMO2 regulated mitochondrial function through interaction with TRIAP1

Flow cytometry was employed to measure ROS levels to investigate the effects of SLMO2 and TRIAP1

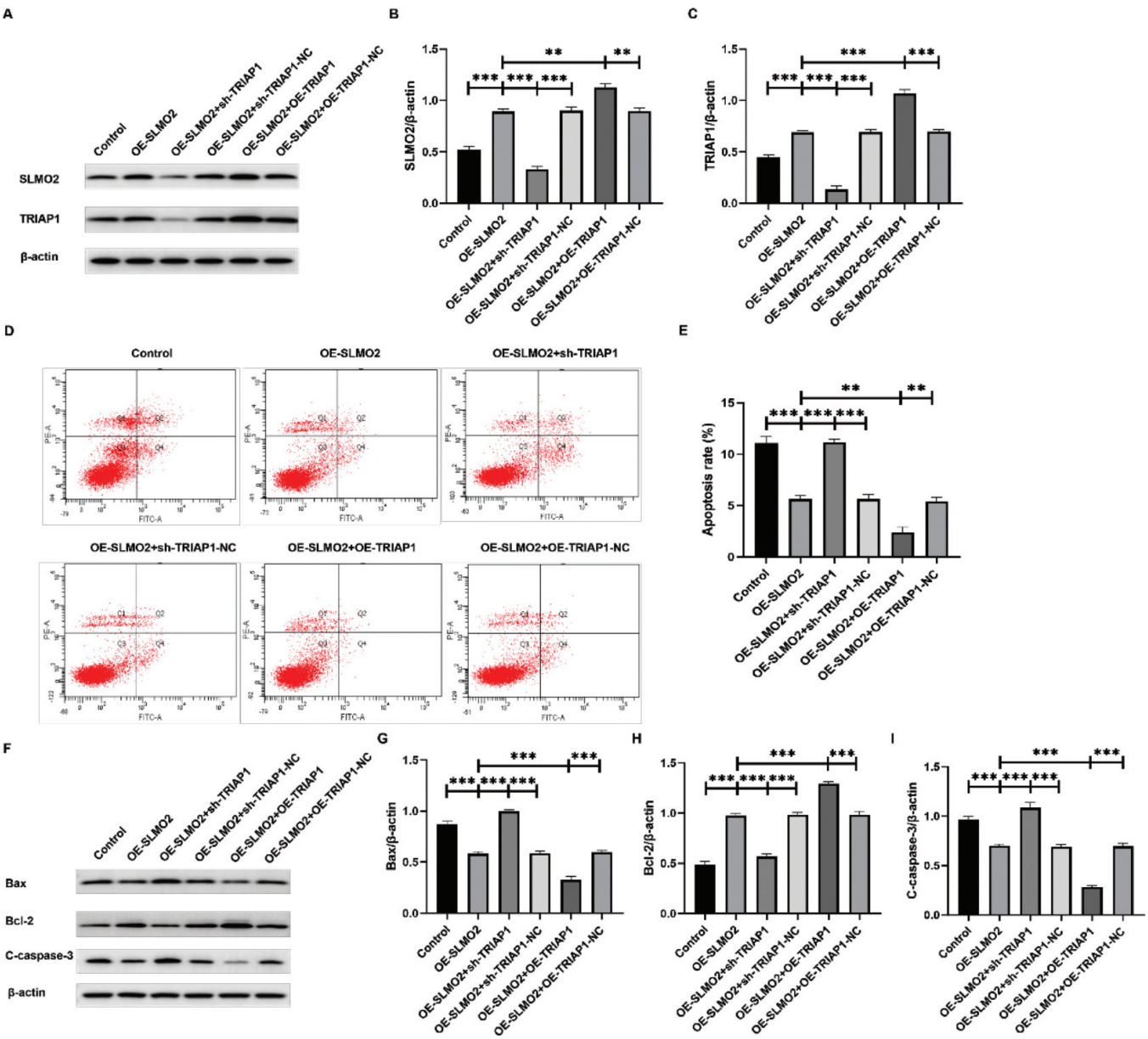

Fig. 4. SLMO2, in combination with TRIAP1, can inhibit apoptosis. **A-C.** Western blot was performed to verify transfection efficiency, and ImageJ was utilized for the quantitative analysis of protein band intensities. **(D, E)** Flow cytometry was employed to evaluate the impact of SLMO2 and TRIAP1 expression on apoptosis in SKOV3 cells. **(F-I)** Western blot analysis was conducted to detect apoptosis-related proteins, and ImageJ was utilized for the quantitative analysis of protein band intensities. n=3, $^{**}p<0.01$, $^{***}p<0.001$.

on mitochondrial function in SKOV3 cells. The results indicated that, compared with the OE-SLMO2 group, ROS levels were significantly increased in the OE-SLMO2+sh-TRIAP1 group, while they were significantly decreased in the OE-SLMO2+OE-TRIAP1 group (Fig. 5A,B). Additionally, western blot analysis further confirmed this observation. Beclin-1, Parkin, and Pink1 expression levels were significantly elevated following TRIAP1 knockdown, while their expression levels markedly decreased with TRIAP1 overexpression (Fig. 5C-F). These results indicated that SLMO2 regulated mitochondrial function through its interaction with TRIAP1.

SLMO2, in combination with TRIAP1, promoted the growth of tumor cells

After conducting *in vitro* experiments to investigate the effects of SLMO2 and TRIAP1 on ovarian cancer cells, we developed an *in vivo* subcutaneous tumor model for further validation. SKOV3 cells were injected subcutaneously into the axillary region of the right forelimb of the mice, and tumor volume was measured and recorded weekly (Fig. 6A). After 28 days, the nude mice were anesthetized and euthanized. The tumors were excised and weighed (Figs. 6B,C). The results indicated that, compared with the control group, the tumor volume significantly increased in the OE-SLMO2 and OE-SLMO2+OE-TRIAP1 groups, whereas it significantly decreased in the OE-SLMO2+sh-TRIAP1 group. Immunohistochemical analysis utilizing Ki-67 as a proliferation marker indicated that SLMO2 and TRIAP1 promoted tumor cell proliferation, further suggesting that their combination inhibited apoptosis (Fig. 6D,E). Additionally, immunohistochemical staining of SLMO2 and TRIAP1 in tumor tissues corroborated these findings (Fig. 6F-H).

In vivo verification of the SLMO2 and TRIAP1 combination regulating mitochondrial function

DHE is a fluorescent probe that can penetrate cell membranes and is specifically oxidized by ROS to produce red fluorescence. DHE was utilized to measure the levels of ROS. The results indicated that, compared with the OE-SLMO2 group, ROS levels were significantly elevated in the OE-SLMO2+sh-TRIAP1 group, while they were significantly reduced in the OE-SLMO2+OE-TRIAP1 group (Fig. 7A,B). These findings suggested that the combination of SLMO2 and TRIAP1

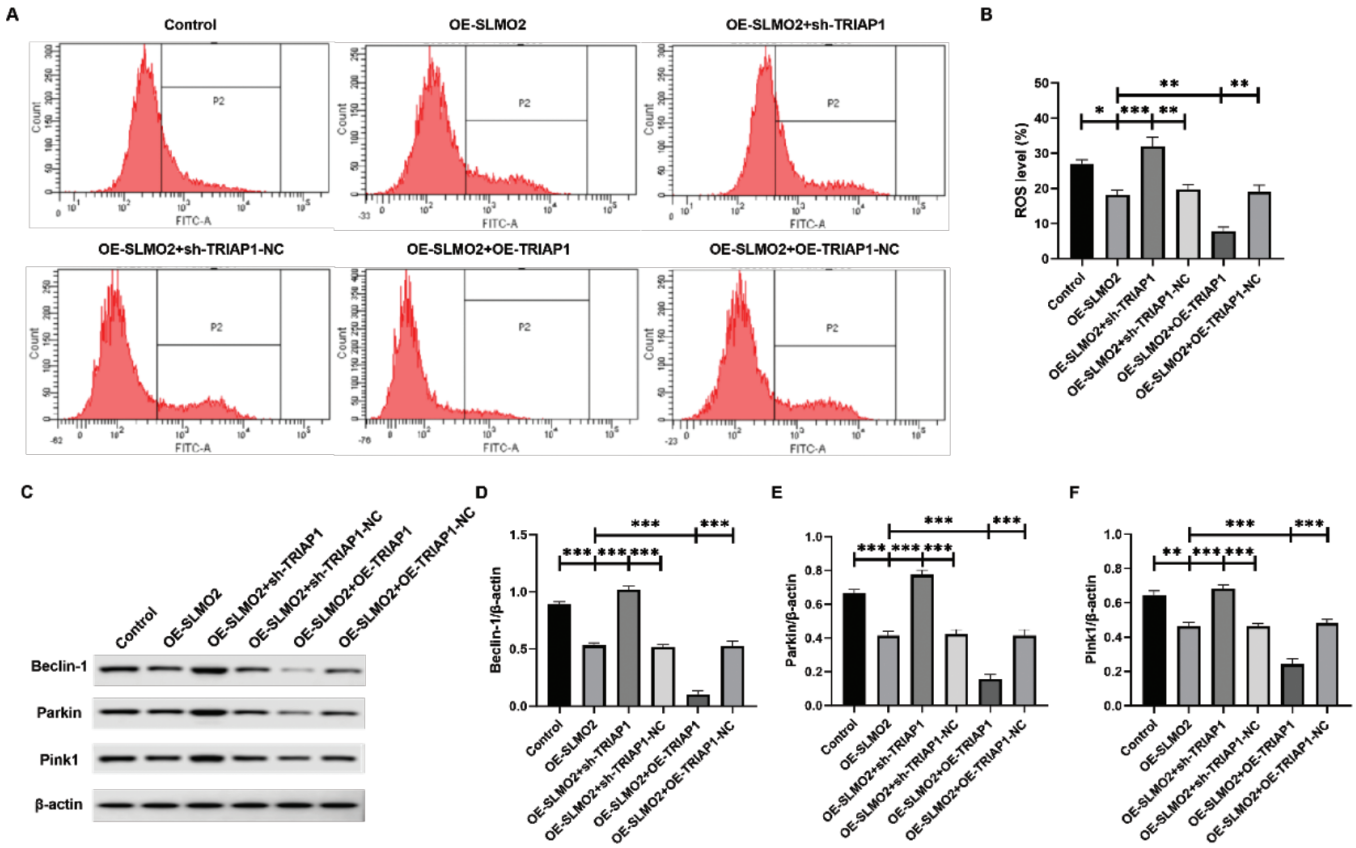

Fig. 5. SLMO2 regulated mitochondrial function through its interaction with TRIAP1. **A, B.** Flow cytometry was employed to measure ROS in SKOV3 cells. **C-F.** Western blot analysis was conducted to evaluate the expression of proteins associated with autophagy and mitochondrial function. ImageJ software was utilized for the quantitative analysis of protein band intensities. n=3, *p<0.05, **p<0.01, ***p<0.001.

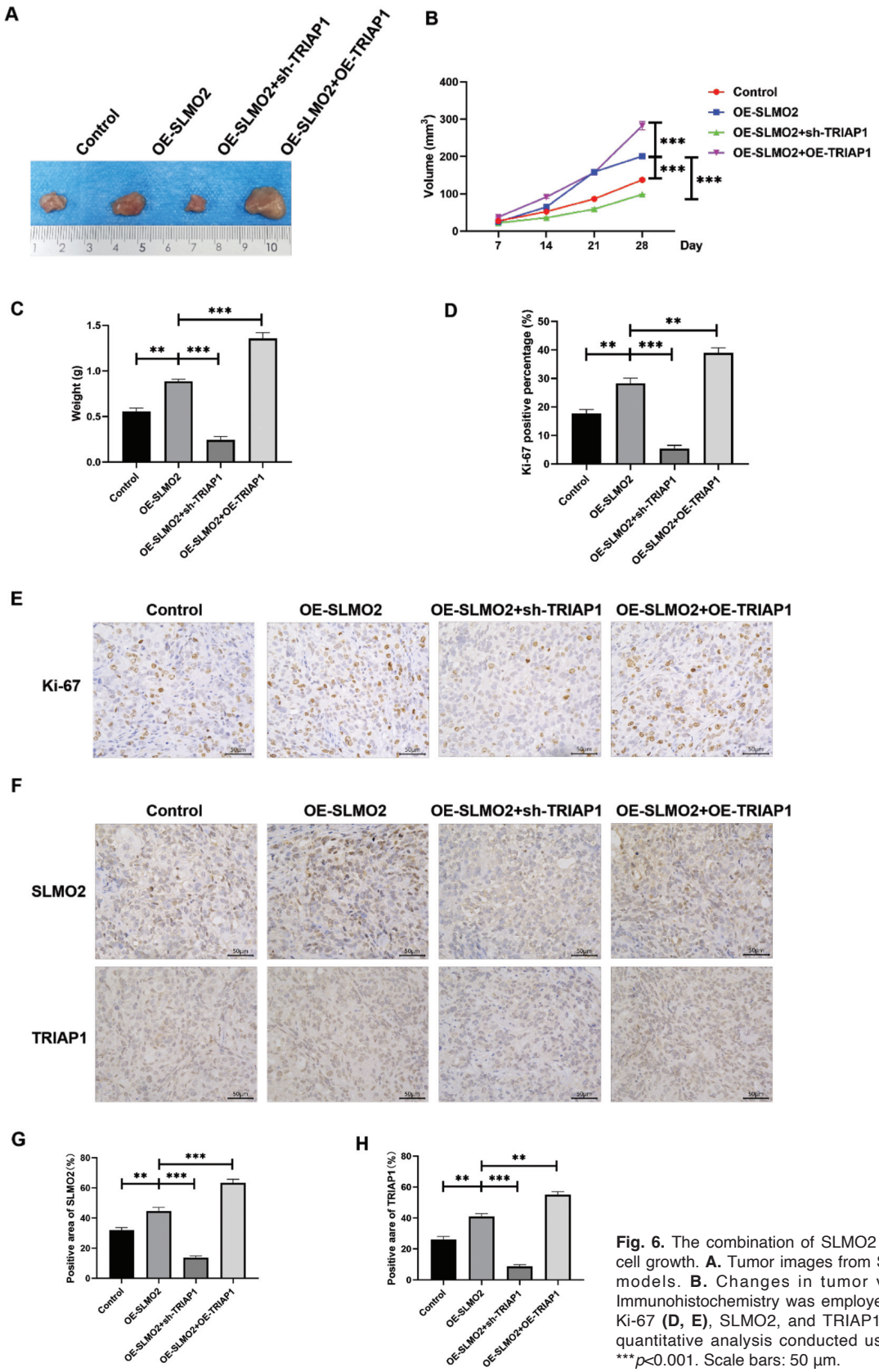

Fig. 6. The combination of SLMO2 and TRIAP1 promoted tumor cell growth. **A.** Tumor images from SKOV3 cell-induced xenograft models. **B.** Changes in tumor volume. **C.** Tumor weight. Immunohistochemistry was employed to detect the expression of Ki-67 **(D, E)**, SLMO2, and TRIAP1 **(F-H)** in tumor tissues, with quantitative analysis conducted using Image J. n=5, $^{**}p<0.01$, $^{***}p<0.001$. Scale bars: 50 μm.

enhanced oxidative stress. The expression levels of Beclin-1, Parkin, and Pink1 were further evaluated using western blot analysis. The results indicated that the synergistic effect of SLMO2 and TRIAP1 inhibited autophagy (Fig. 7C-F). These findings indicated that SLMO2 regulated mitochondrial function by binding to TRIAP1, thereby inhibiting apoptosis in ovarian cancer cells.

Discussion

Ovarian cancer is a particularly challenging malignant tumor in gynecologic oncology, characterized by a high mortality rate. This is primarily due to the absence of noticeable early symptoms, the ease with which the cancer metastasizes, and the limited effectiveness of current treatment methods in certain patients (Armstrong et al., 2022). Therefore, it is essential to thoroughly investigate the molecular mechanisms that contribute to the development of ovarian cancer and to identify new therapeutic targets based on these findings. Such advancements could enhance the prognosis for patients with ovarian cancer. In recent years, the continuous advancement of tumor biology research has led to increased attention on mitochondria, often referred to as "cellular power-

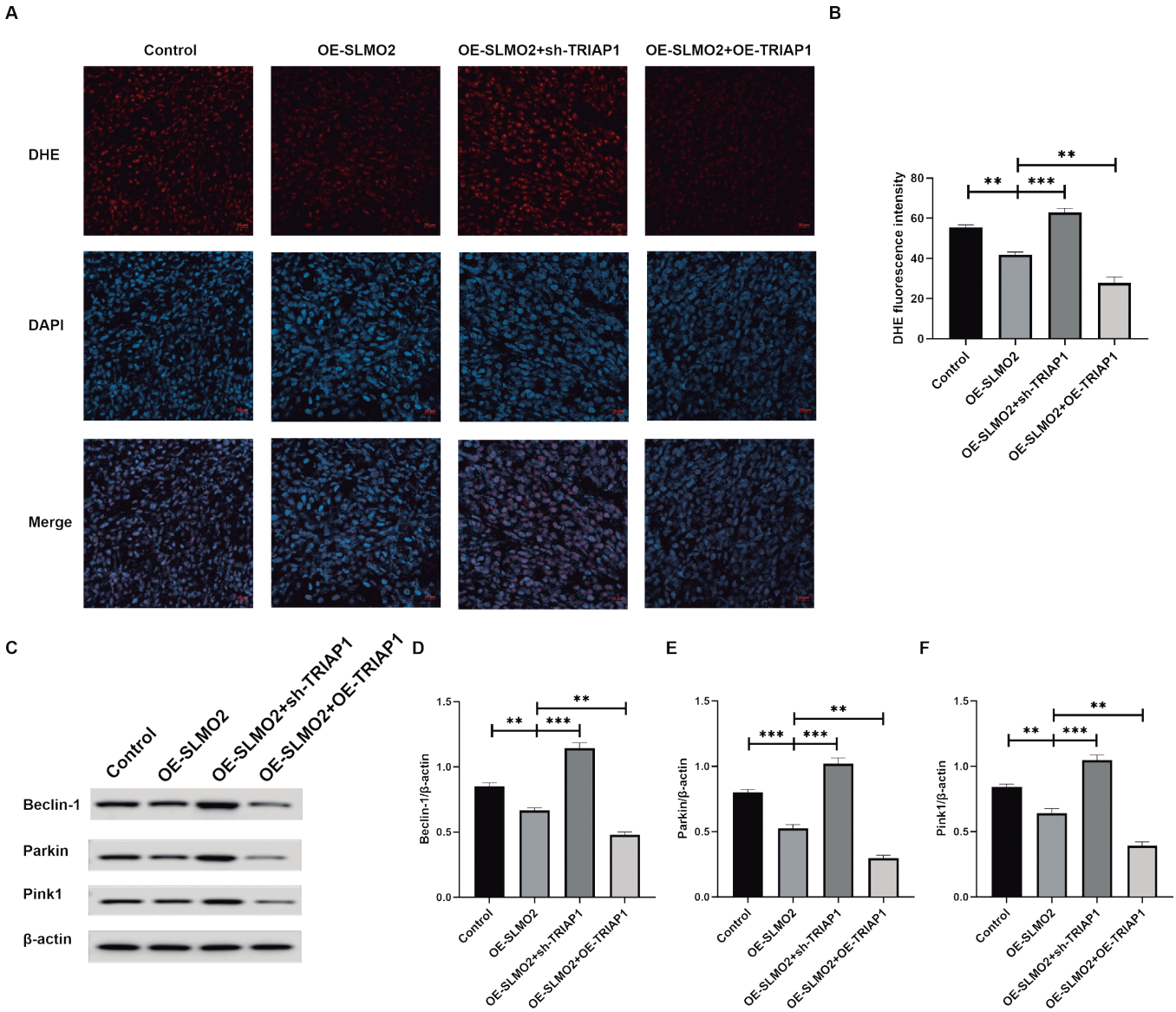

Fig. 7. *In vivo* verification of SLMO2 and TRIAP1 in regulating mitochondrial function. **A, B.** DHE staining was employed to detect ROS levels, and ImageJ was utilized for quantitative fluorescence analysis. **C-F.** Western blotting was conducted to assess the expression of proteins associated with autophagy and mitochondrial function, utilizing ImageJ for the quantitative analysis of protein band intensity. n=5, **p<0.01, ***p<0.001. x 200.

houses", for their roles in tumorigenesis, development, and drug resistance (Missiroli et al., 2020; Vasan et al., 2020). Mitochondria are not only the primary sites of cellular aerobic respiration and ATP production, but they also play significant roles in regulating essential cellular processes, including apoptosis, calcium homeostasis, and metabolic reprogramming (Abate et al., 2020; Kawano et al., 2023; Zheng et al., 2023). In tumor cells, mitochondrial dysfunction is widely recognized as a key factor contributing to tumor progression and drug resistance (Ma et al., 2023).

Among the various molecules that regulate mitochondrial function, mitochondrial lipid transport proteins, such as SLMO2, are increasingly gaining attention in research (Liu et al., 2014). SLMO2 preserves membrane stability and dynamic homeostasis by interacting with mitochondrial membrane lipids (Wei et al., 2015). It also plays a crucial role in lipid metabolism and lipid-associated signaling, influencing mitochondrial energy metabolism, the oxidative stress response, and the regulation of apoptosis (Dee and Moffat, 2005). These functions make SLMO2 essential for maintaining mitochondrial function and cellular homeostasis, which has garnered significant interest in the study of diseases associated with metabolic abnormalities, such as cancer. In this study, we employed lentiviral infection techniques to stably overexpress or knock down the *SLMO2* gene in ovarian cancer cell lines. The experimental results indicated that the overexpression of SLMO2 significantly inhibited apoptosis in ovarian cancer cells, increased mitochondrial membrane potential, and reduced ROS levels. By maintaining mitochondrial membrane potential, SLMO2 enabled ovarian cancer cells to inhibit apoptosis, thereby promoting tumor cell survival and growth. These results align with previous studies, which indicated that SLMO2 plays a critical role in oxidative stress and apoptosis by maintaining mitochondrial membrane stability, modulating ROS levels, and influencing mitochondrial autophagy. Its effects include inhibiting mitochondrial damage and apoptosis, reducing the need for cellular autophagy, and preventing oxidative stress injury by decreasing excessive ROS accumulation. This positions SLMO2 as a crucial regulator in the processes associated with cell survival in mitochondria.

TRIAP1 also plays a role in regulating phospholipid transport as a component of the mitochondrial intermembrane phosphatidic acid transport complex, which facilitates the transport of phosphatidic acid between mitochondrial membranes (Potting et al., 2013). Studies have shown that the SLMO2-TRIAP1 complex functions as a specific lipid transfer protein within the mitochondrial intermembrane space (Miliara et al., 2023). It facilitates the transport of phosphatidic acid from the endoplasmic reticulum to the inner mitochondrial membrane, where it is subsequently converted into cardiolipin through enzymatic reactions (Sardar et al., 2022). Impairment of phosphatidic acid transport and a reduction in cardiolipin levels can disrupt mitochondrial function and morphology, thereby increasing the risk of cell apoptosis (Huang and Freter, 2015; Li et al., 2015). Our study demonstrates that SLMO2 inhibits cell apoptosis by interacting with TRIAP1. When TRIAP1 was knocked out, the rate of cell apoptosis significantly increased. Conversely, its overexpression, in conjunction with SLMO2 binding, further inhibited apoptosis.

In addition to inhibiting apoptosis, our study also investigated the regulatory role of the SLMO2-TRIAP1 complex on autophagy. Autophagy is a crucial process that maintains cellular homeostasis by degrading and recycling damaged cellular organelles and proteins within the cell (Glick et al., 2010). In cancer cells, autophagy serves dual roles: it can promote cell growth, while excessive activation may lead to cell death (Levy et al., 2017). Our study demonstrated that SLMO2, by binding to TRIAP1, reduced the expression of proteins related to autophagy. This inhibition of autophagy prevented the degradation of damaged mitochondria, thereby preserving mitochondrial function and further enhancing the survival of ovarian cancer cells. *In vivo* experiments utilizing subcutaneous heterologous tumor mouse xenograft models further validated these findings. Our study reveals the significant role of mitochondrial regulation in ovarian cancer and suggests that the SLMO2-TRIAP1 combination may serve as a potential therapeutic target for modulating apoptosis and promoting tumor growth. Importantly, while we established the tumor-promoting role of the SLMO2-TRIAP1 complex, we did not investigate strategies to therapeutically disrupt this interaction. Future studies could concentrate on identifying small molecules, peptides, or RNA-based therapeutics that specifically inhibit the binding of SLMO2 to TRIAP1. This inhibition may disrupt mitochondrial homeostasis and sensitize ovarian cancer cells to apoptosis. Structural analysis of the complex using cryo-electron microscopy (cryo-EM) or molecular modeling could enhance drug design by elucidating critical binding interfaces. Moreover, treatment strategies that combine SLMO2-TRIAP1 disruption with standard chemotherapy may improve therapeutic outcomes, particularly in chemoresistant subtypes of ovarian cancer.

This study primarily focused on cell and mouse models without validating its findings with clinical samples, which may limit its relevance for practical clinical applications. Second, this study primarily evaluated the effects of SLMO2 and TRIAP1 on cell proliferation and apoptosis in the short term, but it lacked an assessment of long-term effects, including the potential for tumor resistance and metastasis. In conclusion, this study highlighted the essential role of SLMO2 in preserving mitochondrial function and inhibiting apoptosis in ovarian cancer cells by binding to TRIAP1. The binding of SLMO2 and TRIAP1 promotes tumor growth and oxidative stress, positioning them as potential targets for therapeutic intervention. Future research should concentrate on developing strategies to

disrupt the SLMO2-TRIAP1 complex and investigate its potential for combination with existing cancer treatments to enhance outcomes for patients with ovarian cancer.

Conclusions

SLMO2 regulated mitochondrial function and inhibited apoptosis in ovarian cancer cells by interacting with TRIAP1. The combination of SLMO2 and TRIAP1 promoted tumor cell growth and induced oxidative stress, presenting potential therapeutic targets for ovarian cancer.

Acknowledgements. We appreciate funding support from the Yantai Science and Technology Innovation Development Plan

Funding. This work was supported by the Yantai Science and Technology Innovation Development Plan (Project No: 2022YD065).

Ethics approval and consent to participate. The animal experiment was approved by the Animal Ethics Committee of Yantai Mountain Hospital, and strictly followed EU regulations on the handling and use of experimental animals and operating in accordance with ARRIVE's guidelines for reporting experiments involving animals.

Availability of data and materials. The data supporting the findings of this study are available from the authors, however, restrictions apply. These data were used under license for the current study and are not publicly available. Data are, however, available from the authors upon reasonable request and with permission from the authors.

Authors' contributions. Yaqi Wang: Conceptualization, Methodology, Writing–original draft. Yuesong Wang: Conceptualization, Formal Analysis, and Visualization. Zixuan Li: Formal analysis, Supervision, Writing–review and editing. Tianmei Zhang: Conceptualization, Funding acquisition, Writing–review and editing.

Competing interests. The authors declare that the research was conducted in the absence of any commercial or financial relationships that could be construed as a potential conflict of interest.

References

Aaltonen M.J., Friedman J.R., Osman C., Salin B., di Rago J.-P., Nunnari J., Langer T. and Tatsuta T. (2016). MICOS and phospholipid transfer by Ups2-Mdm35 organize membrane lipid synthesis in mitochondria. J. Cell Biol. 213, 525-534.

Abate M., Festa A., Falco M., Lombardi A., Luce A., Grimaldi A., Zappavigna S., Sperlongano P., Irace C., Caraglia M. and Misso G. (2020). Mitochondria as playmakers of apoptosis, autophagy and senescence. Semin. Cell Dev. Biol. 98, 139-153.

Armstrong D.K., Alvarez R.D., Backes F.J., Bakkum-Gamez J.N., Barroilhet L., Behbakht K., Berchuck A., Chen L.-M., Chitiyo V.C., Cristea M., DeRosa M., Eisenhauer E.L., Gershenson D.M., Gray H.J., Grisham R., Hakam A., Jain A., Karam A., Konecny G.E., Leath III C.A., Leiserowitz G., Liu J., Martin L., Matei D., McHale M., McLean K., Miller D.S., Percac-Lima S., Remmenga S.W., Schorge J., Stewart D., Thaker P.H., Vargas R., Hendrickson A.W., Werner T.L., Zsiros E., Dwyer M.A. and Hang L. (2022). NCCN Guidelines® insights: Ovarian cancer, Version 3.2022. J. Natl. Compr. Canc. Netw. 20, 972-980.

Bray F., Laversanne M., Sung H., Ferlay J., Siegel R.L., Soerjomataram I. and Jemal A. (2024). Global cancer statistics 2022: GLOBOCAN estimates of incidence and mortality worldwide for 36 cancers in 185 countries. CA Cancer J. Clin. 74, 229-263.

Dee C.T. and Moffat K.G. (2005). A novel family of mitochondrial proteins is represented by the Drosophila genes slmo, preli-like and real-time. Dev. Genes Evol. 215, 248-254.

Glick D., Barth S. and Macleod K.F. (2010). Autophagy: Cellular and molecular mechanisms. J. Pathol. 221, 3-12.

Huang C. and Freter C. (2015). Lipid metabolism, apoptosis and cancer therapy. Int. J. Mol. Sci. 16, 924-949.

Kawano I., Bazila B., Ježek P. and Dlasková A. (2023). Mitochondrial dynamics and cristae shape changes during metabolic reprogramming. Antioxid. Redox Signal. 39, 684-707.

Kopinski P.K., Singh L.N., Zhang S., Lott M.T. and Wallace D.C. (2021). Mitochondrial DNA variation and cancer. Nat. Rev. Cancer 21, 431-445.

Levy J.M.M., Towers C.G. and Thorburn A. (2017). Targeting autophagy in cancer. Nat. Rev. Cancer 17, 528-542.

Li X.-X., Tsoi B., Li Y.-F., Kurihara H. and He R.-R. (2015). Cardiolipin and its different properties in mitophagy and apoptosis. J. Histochem. Cytochem. 63, 301-311.

Liu M., Goss P.E., Ingle J.N., Kubo M., Furukawa Y., Batzler A., Jenkins G.D., Carlson E.E., Nakamura Y., Schaid D.J., Chapman J.-A.W., Shepherd L.E., Ellis M.J., Khosla S., Wang L. and Weinshilboum R.M. (2014). Aromatase inhibitor-associated bone fractures: A case-cohort GWAS and functional genomics. Mol. Endocrinol. 28, 1740-1751.

Liu B.-H., Xu C.-Z., Liu Y., Lu Z.-L., Fu T.-L., Li G.-R., Deng Y., Luo G.-Q., Ding S., Li N. and Geng Q. (2024a). Mitochondrial quality control in human health and disease. Mil. Med. Res. 11, 32.

Liu X., Yuan R., Peng J., Xu A., Nie X., Tang R. and Li G. (2024b). SLMO2 is a potential prognostic and immunological biomarker in human pan-cancer. Sci. Rep. 14, 1070.

Luo Y., Ma J. and Lu W. (2020). The significance of mitochondrial dysfunction in cancer. Int. J. Mol. Sci. 21, 5598.

Ma Z., Han H. and Zhao Y. (2023). Mitochondrial dysfunction-targeted nanosystems for precise tumor therapeutics. Biomaterials 293, 121947.

Miliara X., Tatsuta T., Berry J.-L., Rouse S.L., Solak K., Chorev D.S., Wu D., Robinson C.V., Matthews S. and Langer T. (2019). Structural determinants of lipid specificity within Ups/PRELI lipid transfer proteins. Nat. Commun. 10, 1130.

Miliara X., Tatsuta T., Eiyama A., Langer T., Rouse S.L. and Matthews S. (2023). An intermolecular hydrogen bonded network in the PRELID-TRIAP protein family plays a role in lipid sensing. Biochim Biophys. Acta Proteins Proteom. 1871, 140867.

Missiroli S., Perrone M., Genovese I., Pinton P. and Giorgi C. (2020). Cancer metabolism and mitochondria: Finding novel mechanisms to fight tumours. eBioMedicine 59, 102943.

Miyata N., Ito T., Nakashima M., Fujii S. and Kuge O. (2022). Mitochondrial phosphatidylethanolamine synthesis affects mitochondrial energy metabolism and quiescence entry through attenuation of Snf1/AMPK signaling in yeast. FASEB J. 36, e22355.

Nedara K., Reinhardt C., Lebraud E., Arena G., Gracia C., Buard V., Pioche-Durieu C., Castelli F., Colsch B., Bénit P., Rustin P., Albaud B., Gestraud P., Baulande S., Servant N., Deutsch E., Verbavatz J.-M., Brenner C., Milliat F. and Modjtahedi N. (2022). Relevance of the TRIAP1/p53 axis in colon cancer cell proliferation and adaptation to glutamine deprivation. Front. Oncol. 12, 958155.

Penny S.M. (2020). Ovarian cancer: An overview. Radiol. Technol. 91,

561-575.

Potting C., Tatsuta T., König T., Haag M., Wai T., Aaltonen M.J. and Langer T. (2013). TRIAP1/PRELI complexes prevent apoptosis by mediating intramitochondrial transport of phosphatidic acid. Cell Metab. 18, 287-295.

Sardar A., Dewangan N., Panda B., Bhowmick D. and Tarafdar P.K. (2022). Lipid and lipidation in membrane fusion. J. Membr. Biol. 255, 691-703.

Smits M.A.J., Schomakers B.V., van Weeghel M., Wever E.J.M., Wüst R.C.I., Dijk F., Janssens G.E., Goddijn M., Mastenbroek S., Houtkooper R.H. and Hamer G. (2023). Human ovarian aging is characterized by oxidative damage and mitochondrial dysfunction. Hum. Reprod. 38, 2208-2220.

Vasan K., Werner M. and Chandel N.S. (2020). Mitochondrial metabolism as a target for cancer therapy. Cell Metab. 32, 341-352.

Vringer E. and Tait S.W.G. (2022). Mitochondria and cell death-associated inflammation. Cell Death Differ. 30, 304-312.

Wei Y., Wang Z., Su L., Chen F., Tejera P., Bajwa E.K., Wurfel M.M., Lin X. and Christiani D.C. (2015). Platelet count mediates the contribution of a genetic variant in LRRC16A to ARDS risk. Chest 147, 607-617.

Zhang L., Wu J., Zhu Z., He Y. and Fang R. (2023). Mitochondrion: A bridge linking aging and degenerative diseases. Life Sci. 322, 121666.

Zheng S., Wang X., Zhao D., Liu H. and Hu Y. (2023). Calcium homeostasis and cancer: insights from endoplasmic reticulum-centered organelle communications. Trends Cell Biol. 33, 312-323.

Accepted June 25, 2025